Hindawi
Journal of Advanced Transportation
Volume 2019, Article ID 7308590, 17 pages
https://doi.org/10.1155/2019/7308590

Research Article

Advanced Modeling and Simulation of Vehicle Active Aerodynamic Safety

Krzysztof Kurec[1], **Michał Remer**[1], **Jakub Broniszewski**[1], **Przemysław Bibik**[1], **Sylwester Tudruj**[2] and **Janusz Piechna**[1]

[1] *Warsaw University of Technology, Institute of Aeronautics and Applied Mechanics, Warsaw 00-665, Poland*
[2] *Warsaw University of Technology, Institute of Micromechanics and Photonics, Warsaw 02-525, Poland*

Correspondence should be addressed to Janusz Piechna; jpie@meil.pw.edu.pl

Received 3 August 2018; Accepted 6 January 2019; Published 3 February 2019

Guest Editor: Mihai Dimian

The aim of this study was to extend the safety limits of fast moving cars by the application, in a controlled way, of aerodynamic forces which increase as the square of a car's velocity and, if left uncontrolled, dramatically reduce car safety. This paper presents the methods, assumptions, and results of numerical and experimental investigations by modeling and simulation of the aerodynamic characteristics and dynamics of a small sports car equipped with movable aerodynamic elements operated by an electronic subsystem for data acquisition and aerodynamics active automatic control.

1. Introduction

Currently, the trend to minimize emissions by limiting fossil fuel consumption leads to lighter cars with a low drag coefficient. This situation introduces new challenges for car designers. They need to ensure that stability will be good enough to allow safe driving in all road conditions (wind gusts, moving obstacles, etc.). Studies found in the literature mainly focus on sensitivity to lateral wind. These methods attempt to reproduce the test procedure according to the ISO 12021:2010 standard [1]. However, it is rather rare to take into account the coupling of car dynamics and aerodynamics. Very often, it is assumed that car movement will not affect aerodynamic forces. The study presented in [2] is in contrast to this assumption. The authors have shown that the inclusion of a bidirectional fluid structure interaction can lead to a significant change in the aerodynamics forces.

The development of the quality of highways together with the increase in the potential maximum speed of cars has turned the attention of car designers towards the dynamic features of cars at high speeds. The external shapes of cars are typically optimized for low aerodynamic drag. Unfortunately, such action has drawbacks in the form of car bodies generating aerodynamic lift forces at high speed, together with a decrease in a car's directional stability and reduction of safety limits during fast cornering. The frailty of the car body shape is typically compensated by fixed or movable aerodynamic elements activated at high speed. Typically, such aerodynamic elements have the form of a wing, generating downforce which compensates the lift force generated by the car body. The additional aerodynamic elements generate additional drag, so it is desirable to activate the movable elements only when necessary. Some sports cars such as, for example, the Porsche 918 Spyder [3], have predefined aerodynamic settings for a specific range of speeds which make it possible to either minimize drag or maximize downforce, while the active aerodynamics of the McLaren Senna additionally enables it to shift the aerodynamics balance towards the rear of the car to enhance braking. These two examples relate to a case when the active aerodynamics is used to support the maneuvers performed by the driver. However, with the increased number of different types of sensors [4] that can be mounted on a car, it is possible to design a driver assistance system that is able to evaluate the current road conditions [5] and automatically modify the aerodynamic properties. One example where

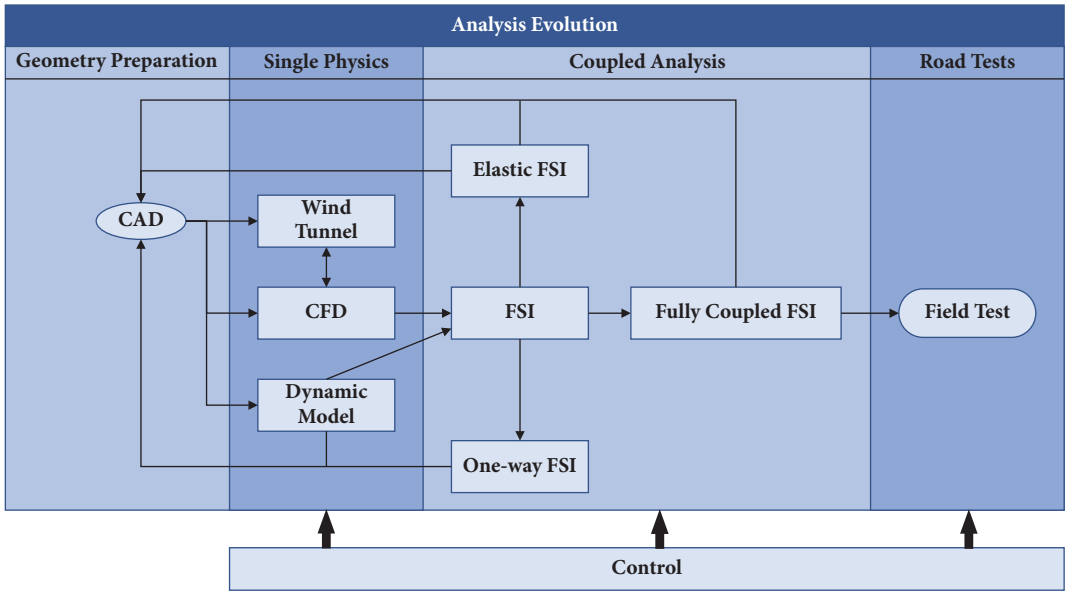

Figure 1: Scheme of the data flow in the project of vehicle active aerodynamic safety, where CAD is computer aided design, CFD is computer fluid dynamics, and FSI is fluid structure interaction.

a driver can be assisted during a rapid maneuver could be the use of machine vision technology to estimate the road curvature [6] and utilize the driving assistance system to assess not only whether the speed is within the safety margin but also whether the vehicle's aerodynamic setup is the most appropriate for the car's safety. This could also give the time essential to perform more significant movements of the active aerodynamic surfaces so that a higher value of the aerodynamic forces can be utilized, even before the driver realizes that some kind of action needs to be taken. The introduction of autonomous driving itself can make it possible to increase safety limits during rapid maneuvers [7]. The development of such systems needs to rely on model based validation due to the costs and complexity, which was emphasized by researchers developing a highway pilot assisting the driver [8].

An aerodynamic active control system requires information about the actual state of the car, the position of the movable aerodynamic elements located on the car body and the steering algorithms. This paper presents information about the methods used for modeling and simulation to develop an active system extending the safety limits of a fast moving car. The electronic control system is the key to the integration of many aspects of scientific and technical activity.

It was considered that information can be collected from sensors located inside the car and that a set of movable aerodynamic elements would be attached to the car body to form a control loop. The control part of the system was assumed to be open for programming taking into account information about the characteristics of the sensors, the actuators and the aerodynamic characteristics of the added aerodynamic elements. The general scheme of data flow in the project is presented in Figure 1.

2. System of Data Acquisition and Active Control of Movable Aerodynamic Elements

A measurement and control system was developed to achieve the project goals. It was decided that, for research purposes, the system should be flexible and easy to modify. The other requirement for the hardware was immunity to vibrations and an ability to work in a broad range of environmental conditions. For those reasons, an industrial real-time controller was selected as the core of the system. The controller was fitted with a set of different types of communication interfaces, which enabled the connection of different sensors and devices. The general architecture of the developed system is presented in Figure 2. The whole system is divided into three subsystems: the measurement subsystem, the actuation (control) subsystem, and the user interface.

The measurement subsystem consists of several sensors together with their interfaces. In the current configuration, all the sensors were connected to the system controller via RS-232C interfaces. The main sensor is an integrated GPS (Global Positioning System) and AHRS (Attitude and Heading Reference System) sensor. This sensor provides navigation and vehicle state data: linear acceleration, linear velocity components, inertial position, angular rates, and attitude angles in three perpendicular axes. All the data was collected at a frequency of 200 Hz. The next sensor is the vehicle control measurement sensor. This sensor provides data of the vehicle steering wheel angle and the throttle and brake pedal positions at a frequency of 100 Hz. These two sensors are sufficient for the control of the vehicle aerodynamic surfaces. For some parts of this research, the system may also use suspension deflection sensors which use linear potentiometer sensors in each of the vehicle shock absorbers.

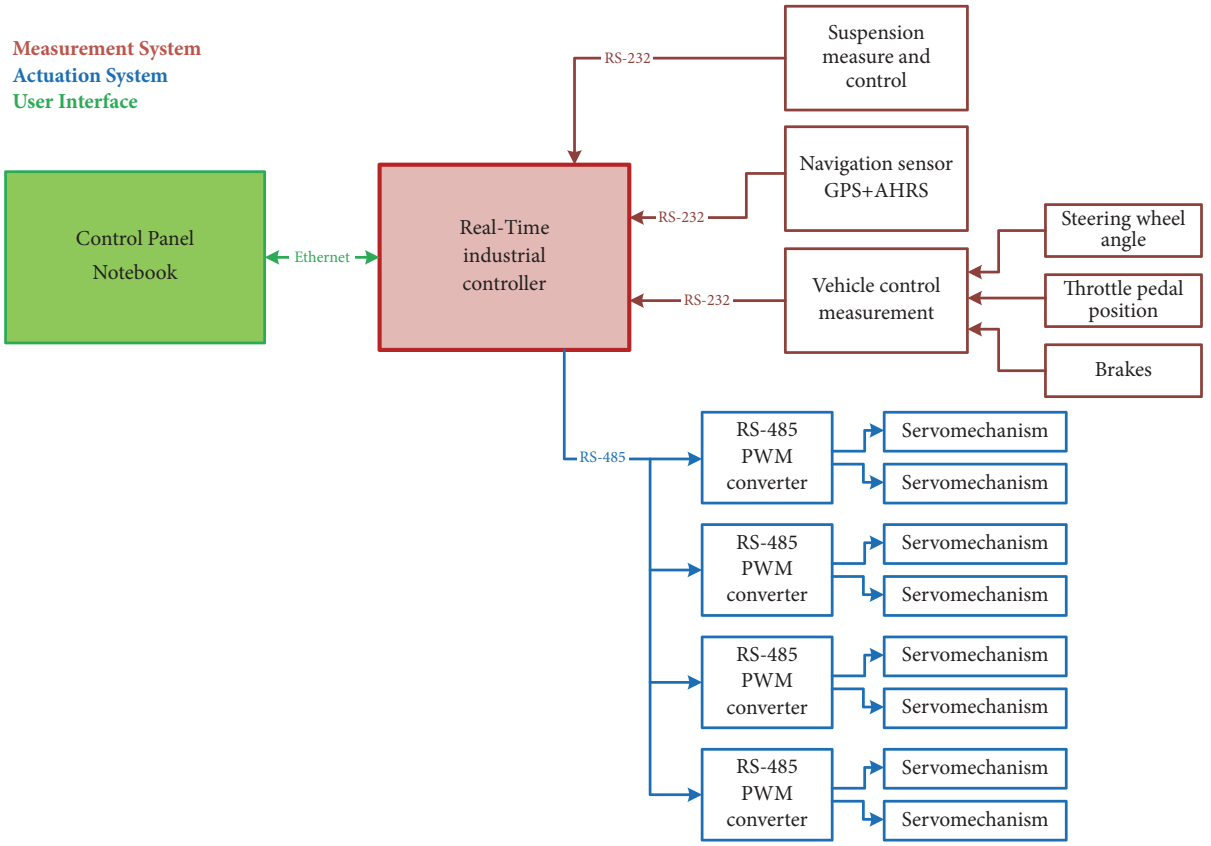

Figure 2: Hardware architecture of the measurement and control system.

The actuation subsystem consists of two parts, actuation of aerodynamic elements and suspension control. The aerodynamic surfaces are fitted with PWM (Pulse Width Modulation) signal controlled servomechanisms. An RS-485 interface is used to control those servomechanisms and all servomechanisms are connected to the RS-485 control line via signals converters. All servomechanisms are controlled at a frequency of 20 Hz.

The third subsystem is the user interface. The GUI is installed on the notebook connected to the system controller via an Ethernet interface. The GUI allows the operator to observe the measurement data, configure the controller (different modes of operation are possible), and manually control the aerodynamic surfaces. The RT controller may also be configured to operate in a fully automatic way without the user control interface panel connected.

The system software was developed using National Instruments LabVIEW software. The main objective of the application was to ensure real-time operation of the system. Several parallel modules are defined in the architecture of the software (see Figure 3). The system processes module is responsible for governing the operation of the system. The user interface communication module exchanges data with the user control panel by sending sensor readings and receiving commands and instructions from the user. The data acquisition module ensures communication with the sensors and is responsible for the synchronous reading of

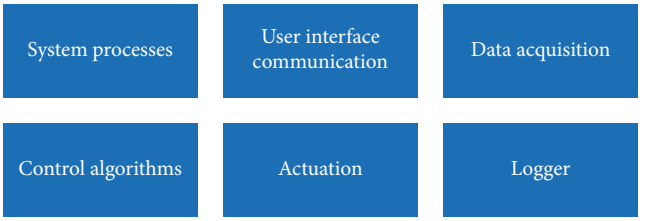

Figure 3: System software modules.

data from all sensors. The control algorithms module receives data from the data acquisition module and processes the data according to defined control laws and sends commands to the actuation module which then sends the commands to all control elements. The logger module records both data from all sensors and all control commands during operation of the system.

3. Models and Simulations

The aim of the presented study was to extend the safety limit of a fast moving vehicle in conditions of strong changes to the atmospheric and physical environment and the rapid reactions of the driver. Widely used ESP systems for vehicle stabilization use forces generated during braking of selected

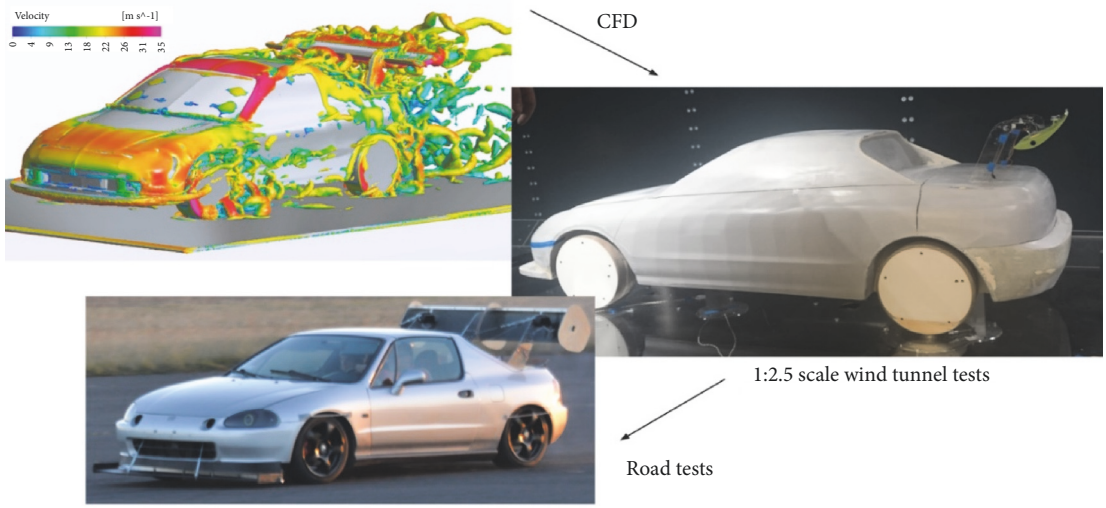

Figure 4: The three different types of aerodynamic study.

vehicle wheels. In this analysis, it is proposed to use aerodynamic forces for this purpose. The results of the active actions of moving aerodynamic elements aimed at stabilizing vehicle motion are discussed below. During the development of a new aerodynamic solution, it is necessary to identify the problems to be solved and the tools needed to achieve the goal. The final solution should be tested in real life on a test car; however, a wide range of modeling techniques can be utilized to aid development.

3.1. The Use of a Variety of Different Modeling Techniques. In the analyzed case, the objective is to actively control the aerodynamic properties of a light sports car such as the Honda CRX del Sol. It was recognized that the conclusions resulting from the flow analysis of this car could be extended to many other high-speed designs. The geometry of this car is presented in Figure 4 which shows the car used during track tests together with its wind tunnel model and CAD model incorporated into the CFD calculations.

The most important data was recorded during the test rides and gave the answer to the question of which aerodynamic setups were the most efficient to control the car's dynamics, while the results from the CFD calculations were used to complement the data acquired during wind tunnel tests and were used to gain additional knowledge of the nature of the flow around the car body. Each of the described actions is shown in Figure 4 to emphasize the fact that a very wide range of data can be obtained by employing them all together. The use of modeling techniques makes it possible to study many different scenarios, including scenarios that could be dangerous to test on a real car.

Below, a brief review of the modeling techniques used is presented, starting with the wind tunnel tests through to the different kinds of modeling based on CFD calculations. In each consecutive case, the CFD calculations were expanded by additional elements. In most cases of traditional automotive aerodynamics, stationary and solid bodies are being investigated. This paper describes more advanced techniques that are essential to accurately predict the behavior of a car subjected to active control by moving aerodynamic surfaces. This includes studies of such cases as the movement of the rear wing, the behavior and influence of deformable surfaces attached to the car body, as well as a complete simulation of a moving car. Apart from the simulations, the development of an algorithm enabling the control of moving aerodynamic elements is presented as well.

To carry out the proposed activities, the following software was selected:

(1) to construct the 3D geometry of a vehicle and moving aerodynamic elements installed on its body; it was assumed that SolidWorks, Unigraphics software, and software included in the ANSYS-Fluent package would be used;

(2) for vehicle body flow analysis; it was assumed that CFD ANSYS-Fluent commercial software would be used together with the freely available OpenFOAM software;

(3) for vehicle dynamics; it was assumed that MCS.Adams/Car would be used alongside Matlab/Simulink as an interface between MCS.Adams and ANSYS-Fluent;

(4) in-house software for analyzing the motion of deformable elastic car body parts and simulating the dynamics of vehicle body motion.

Taking into account the multidisciplinary problems accompanied by the main and general problem, some new ideas of transferring expert knowledge to the engineering level can be applied. An example is the SORCER software [9] used by some team members for the solution of other problems. The idea of preparing software blocks by experts to solve separate detailed problems and integrating individual solutions into a bigger and wider problem consideration is the basis of the SORCER software. Due to the personal limitation of the team

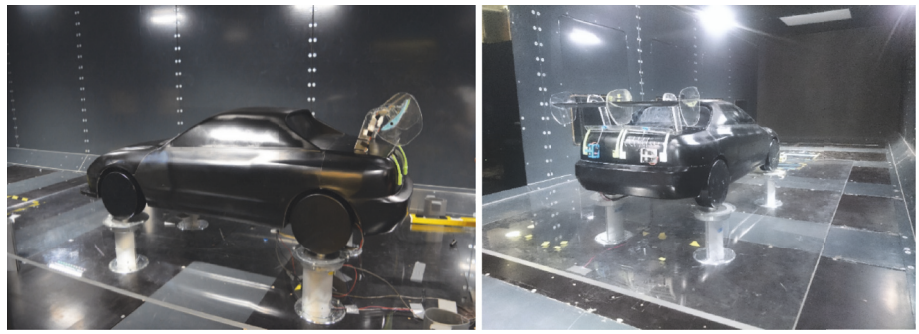

Figure 5: Model of the vehicle in the wind tunnel.

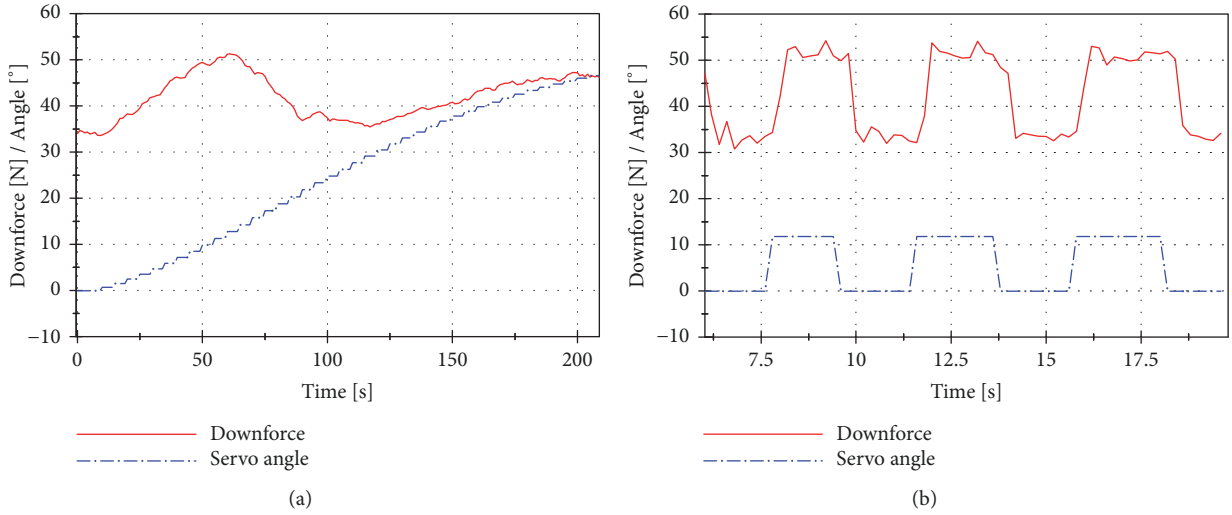

Figure 6: Characteristics of the downforce and the servo angle for (a) a slow movement of the wing and (b) quick changes of the wing's placement from -5° up to 50°.

engaged in problem development it was finally decided to use a more conventional approach.

3.2. Investigations of the Flow in the Wind Tunnel on a Scaled Down Model. As the flow around a vehicle equipped with additional aerodynamic surfaces has a sophisticated nature, experimental fluid mechanics is the best way to acquire knowledge about the aerodynamic forces acting on a car body. In the presented study, the experimental measurements of the aerodynamic forces were collected during the wind tunnel tests performed on a model of the Honda CRX del Sol. The model of the car body was prepared at a 1:2.5 scale and was thoroughly tested in the wind tunnel at an inflow velocity of 23 m/s and at a turbulence intensity equal to 3.5%, whereas the Reynolds number exceeded two million. The experimental set-up was equipped with four load cells, each installed below a wheel of the vehicle, measuring appropriate forces and momentums. The model was laid on a separation plate to reduce the influence of the boundary layer generated on the wind tunnel's walls [10], as can be seen in Figure 5. The model was tested for various configurations, starting with a clean body, without any additional aerodynamics surfaces, and finishing with over six surfaces provided with servomechanisms. Additionally, the flow was visualized with the use of a Ti_2O oil mixture and minitufts. The results obtained for the clean configuration (see Figure 7) were the reference for further more complicated geometrical configurations, also calculated by means of numerical fluid mechanics. Such a configuration makes it possible to receive both time dependent results for force values and typical static measurements, which were recalculated to nondimensional coefficients of downforce (see Figure 8) and drag force (Figure 8).

The other feature of the wind tunnel results, apart from the ability to study the characteristics of a stationary rigid geometry, is the ability to perform tests of fast and time dependent changes of the airfoil and spoiler attached to the model of the car. Moreover, the typical characteristic of downforce coefficient as a function of the angle of attack is presented (see Figure 8(a)), and information about the forces as a function of time are also provided. The flow response to the vehicle aerodynamic configuration changes is presented in Figures 6(a) and 6(b). The maximum increase of the downforce is generated in less than two seconds for the wing movement from about 20° to the value of maximum angle of attack. Several configurations were tested achieving a

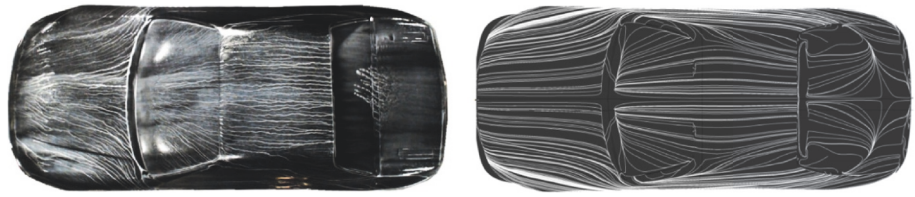

Figure 7: Comparison of the experimental visualization of the oil flow over a clean configuration of the car body (left) and from the CFD calculations (right).

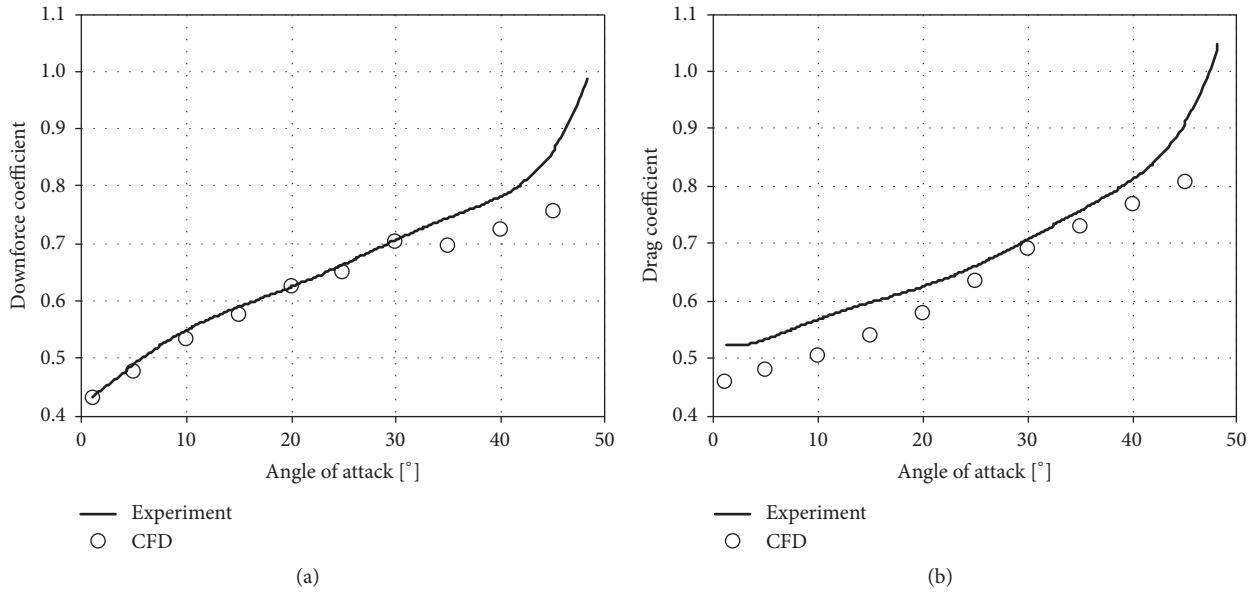

Figure 8: Characteristics of (a) the downforce coefficient and (b) the drag coefficient obtained during the wind tunnel measurements of a car with a mounted rear wing and a spoiler, compared with the CFD results acquired for a wide range of angles of attack.

minimum time to reach maximum increase of the downforce in around 0.6 seconds by the movement of a special spoiler.

3.3. Validation of the CFD Calculations. The values of the aerodynamic forces, as well as some of the flow features recorded during wind tunnel testing, were used to perform validation of the CFD methods. A comparison of the flow features on the surface of the car body is presented in Figure 7, whereas in Figure 8 the values of the downforce coefficient together with the drag coefficient obtained during the experiments and the CFD calculations are presented together. It was established that, for a wide range of studied cases, the SST k-ω turbulence model [11] makes it possible to achieve CFD results close to the experimental data. As can be observed in Figures 7 and 8, a good agreement with the wind tunnel tests was achieved. The SST k-ω turbulence model is one of the most commonly used turbulence models in the field of automotive aerodynamics [12], however, it is best practice to check it for every specific case being studied.

3.4. The Unsteady Aerodynamics: The Search for the Flow Response Time to the Movement of the Active Aerodynamic Elements. One of the most commonly used active aerodynamic elements in the field of the automotive design is a rear wing [13]. The main advantage of such a device is its high efficiency, which makes it possible to achieve a high downforce in a trade-off for a relatively low increase of drag. The rear wing is mounted near the trunk at such a distance from the rest of the car body so that it should not create any negative aerodynamic interferences with the car's silhouette. The area of the wing is proportional to the forces that it can generate, so the larger the wing the higher the values of downforce that can be achieved. Unfortunately, the addition of the rear wing can be seen as a disturbance of a car's aesthetics which leads designers to reduce its size, or to create a mechanism to enable the wing to hide within the car's silhouette or even to completely remove it. Currently, most sports cars have some sort of rear wing, which is used to enhance the car's handling at high speeds. In the case of some cars, for example, the Bugatti Veyron, the rear wing also works in braking mode, by rotating to a high angle of attack, creating additional drag that slows the car down.

If the rear wing is designed to be an active aerodynamic element, apart from its aerodynamic characteristics, it is very important to know how it will be controlled and adjusted to

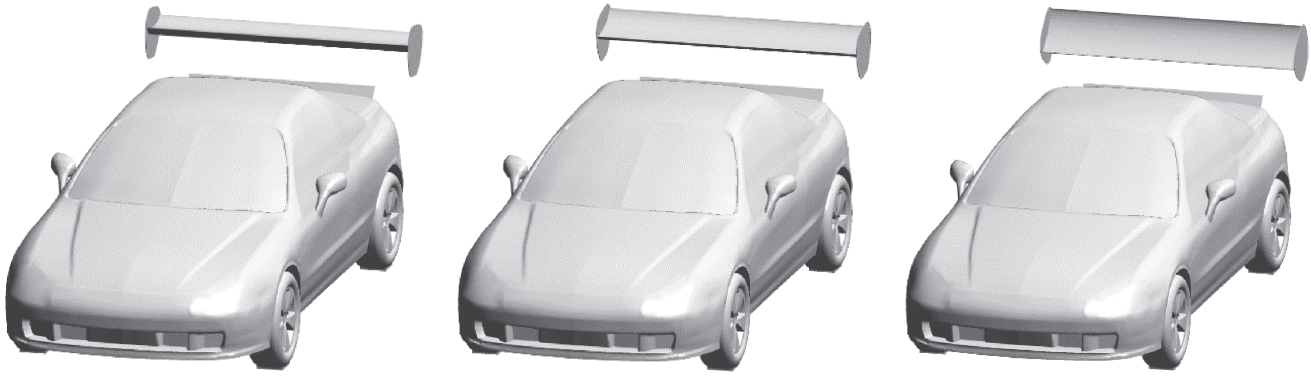

(a) (b) (c)

Figure 9: The car body with the rear wing set to the three different angles of attack: (a) 0°, (b) 20°, and (c) 50°.

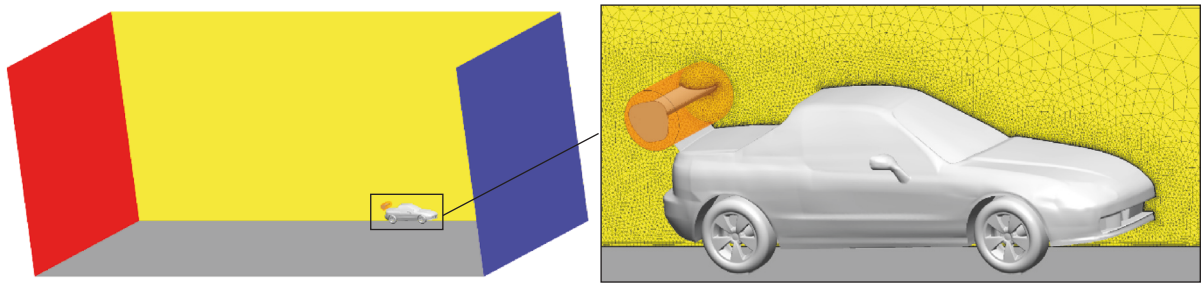

(a) (b)

Figure 10: (a) Geometry of the computational domain. (b) Close-up on the car body with mesh on the symmetry plane.

the desired angle of attack or moved to a specific location relative to the car's silhouette. For this purpose, in this research, it was decided to use electric servomechanisms due to their ability to perform fast movements that allow adjustments of the car's aerodynamic properties in a short time.

The aim of the study presented in this section was to show the unsteady flow features developing over time due to a change of the rear wing's angle of attack (see Figure 9). This research was performed by means of CFD calculations in ANSYS Fluent. Due to the analysis of the unsteady phenomena, a transient solver was utilized together with the SST k-ω turbulence model. Two cases were studied. The first case was for the change of the rear wing's angle of attack from 0° to 20°, which corresponds to a scenario in which an additional downforce needs to be generated by the car body to improve the car's handling. The second case was for the change of the angle of attack from 0° to 50°, which significantly increases not only the downforce but also the drag force by raising the frontal area of the car by 14%, which is beneficial during braking maneuvers. The most important difference between those two cases is that for the change of the angle of attack to 20°, the flow only slightly adjusts to the new orientation of the rear wing, whereas for the case in which the angle of attack is changed to 50°, the flow separates from the wing right at its tip, which creates a separation zone behind it.

The 1:1 scale model of the Honda del Sol was studied within the flow field of the velocity equal to 40 m/s. The domain used in the CFD calculations is presented in Figure 10(a), whereas a close-up of the car itself can be seen in Figure 10(b). The mesh consisted of 11 million tetrahedral elements. The use of the symmetry boundary condition made it possible to perform the calculations only on half of the geometry and thus reduce the total number of elements. To make it possible to change the rear wing's angle of attack, the whole wing together with the side plate was placed inside a cylinder. The cylinder was connected with the rest of the computational domain via a sliding interface. To enable the use of this kind of interface, the rear wing could not include any elements directly connected with the car body. For this reason, the rear wing's mounting was not included in the model. However, the mountings designed for the test car had a "swan shape", which minimized their influence on the downforce generated on the wing, and their omission from the CFD model should not lead to significant discrepancies.

The change of the rear wing's angle of attack over time is depicted in Figures 11(a) and 11(b), the angular velocity of the wing's rotation is the same for both studied cases, which results in the wing reaching an angle equal to 20° in 0.1 s

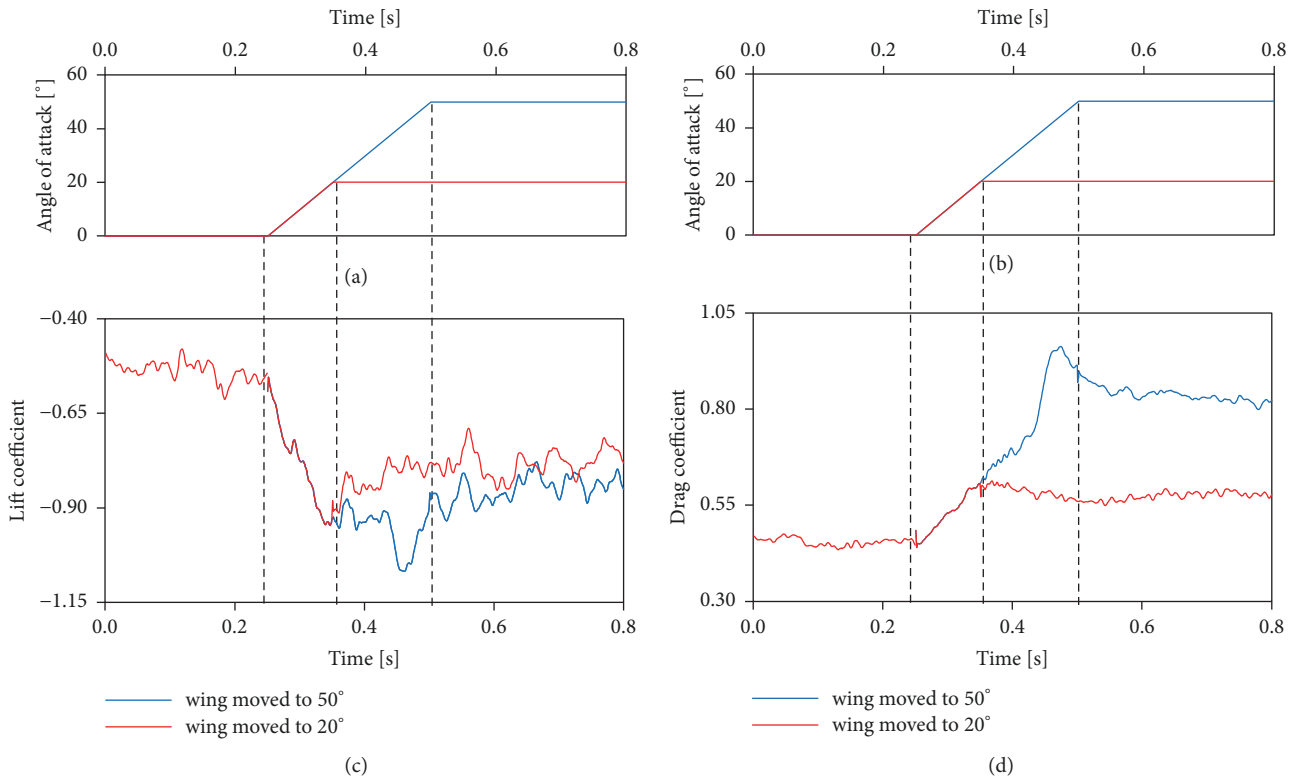

Figure 11: (a), (b) Plots of the rear wing's angle of attack. (c) The characteristics of the lift coefficient over time. (d) The characteristics of the drag coefficient over time.

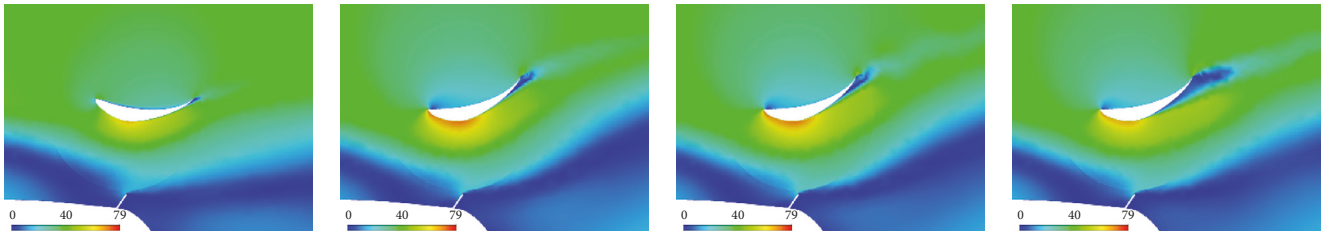

Figure 12: Contours of the velocity in the symmetry plane while the wing is moved to 20° at the following time frames: (a) 0.25 s, (b) 0.35 s, (c) 0.40 s, and (d) 0.45 s.

whereas it takes another 0.15 s for it to rotate up to 50°. The characteristics of the lift coefficient and the drag coefficient (see Figures 11(c) and 11(d)) are the same until 0.35 s, which is the time frame when the wing which was rotated to 20° stops moving and the flow conditions for this case stops changing, whereas for the other case, the wing stops rotating at 0.50 s. In both cases, it takes approximately 0.5 s after the wing stops moving for the flow to fully adapt. It should be noted that, due to the unsteady phenomena, the peak of the absolute values of the lift coefficient as well as the drag coefficient are higher than when the flow settles down, which means that with the fast movement of the active aerodynamic elements it is possible to generate an additional aerodynamic force, although only for a very short duration.

The flow features during the different time frames for both of the studied cases are presented in Figures 12 and 13, where it can be seen that the flow only needs to slightly adapt when the wing is set to 20°, whereas after rotation to 50° a recirculation zone is formed behind it and the flow features change significantly. It should also be noticed that there is a spoiler underneath the wing which is redirecting the flow towards it and makes it possible for the air to "stick" to it at higher angles of attack reaching up to 20°.

The data presented above proves that the unsteady phenomena must be taken into account in the control mechanism of the active aerodynamic elements to accurately predict the aerodynamic load that the car body is subjected to.

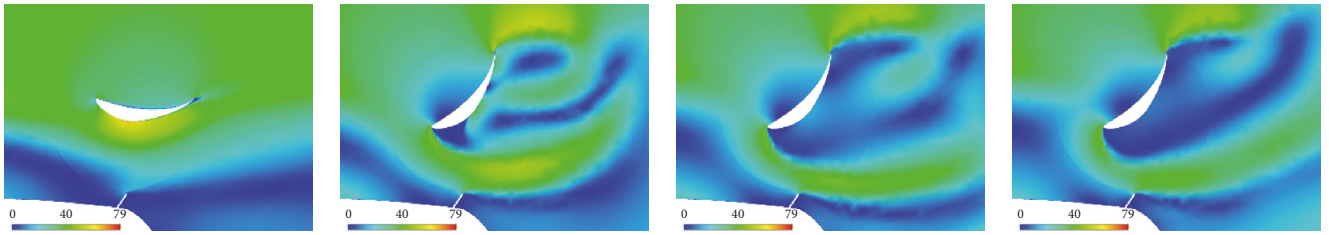

Figure 13: Contours of the velocity in the symmetry plane while the wing is moved to 50° at the following time frames: (a) 0.25 s, (b) 0.50 s, (c) 0.55 s, and (d) 0.60 s.

Table 1: A comparison of the aerodynamic coefficient values for different variants of the tested car model.

	Drag coefficient	Lift coefficient
Base model	0.506	−0.101
Model with an active airbag	0.557	−0.212
Model with an active airbag and side curtains	0.572	−0.312

3.5. Untypical Movable Add-Ons: Elastic Type of the Active Aerodynamic Elements. Typically, rigid elements are used as movable elements. The motion of such an element is achieved by electric servomechanisms with complicated mechanical elements. A pneumatic system of actuation of flexible movable aerodynamic elements was considered. One such solution is presented below.

As described in previous sections of this paper, a rear wing can be used to generate aerodynamic forces, whereas the value of the force is dependent on the wing's angle of attack. A different kind of solution is also proposed in this study, which incorporates the use of flexible deformable surfaces placed in various locations on the vehicle. These deformable surfaces can have the form of airbags, which in an inactive state adhere closely to the body of the vehicle, whereas in an active state (inflated) change their shape and at the same time modify the shape of the vehicle. Such a change in shape would change the value of the aerodynamic forces acting on the car while driving. Controlling the shape of such surfaces consists of supplying compressed air to their interior, and so the material of the airbag stretches and bulges. Once the air is released the elastic resilient material returns to its original shape, adhering to the car's body. The vehicle model tested was equipped with a splitter partially blocking the inflow of air under the car. The main deformable element used was an airbag placed under the splitter. Additionally, to increase its efficiency, deformable side curtains were used [14], whose task was to block the inflow of air under the car from the outside, i.e., from the external environment (see Figure 14(a)).

It was assumed that compressed air would be used to control the shape of the flexible aerodynamic elements with a much higher pressure when compared with the ambient pressure. Thanks to this, these elements would have a fixed shape, regardless of the speed at which the car moves. To determine the shape that the inflated pneumatic side curtains and the airbag under the splitter would take, FEM numeric simulation was performed using the ANSYS software. The surface of the deformable elements was loaded with air at constant pressure, under which they assumed the target shape (see Figure 14(b)). It was assumed that the shape changes associated with the dynamic pressure acting on these elements are negligibly small. The values of the forces and aerodynamic coefficients acting on the car were obtained by means of CFD based numerical simulation using the OpenFOAM software (see Figure 14(c)). The results obtained (see Table 1) confirm the possibility of using flexible deformable elements attached to the car to control the value of the downforce acting on it.

To prepare an appropriate algorithm to control the position of aerodynamic movable elements, it is necessary to predict the way these elements change the motion of a car equipped with such elements. To perform such tests, separate software modeling the dynamics of the car influenced by additional aerodynamic elements was designed.

3.6. Numerical Simulation of Car Dynamics Influenced by the Active Aerodynamic Elements. On the one hand, road test data are the deciding data but, on the other hand, the car dynamics are influenced by a lot of unpredictable factors such as tire pressure and temperature, mistakes in suspension geometry, side wind, road inclination, predisposition of the driver, etc. Therefore, independent software for car dynamic analysis was developed and validated by comparison with known solutions [15–17].

Information about the aerodynamic characteristics of the car body had to be transferred to the car dynamic analysis software to check the influence of the proposed modifications. The intention was to have the model with all mechanical coefficients precisely defined and check the car's reaction only for the chosen parameters.

The 6DOF (six degrees of freedom) car dynamic model that was developed employed the Segel model of lateral forces generated by the tire [17, 18]. This model is relatively old (it was developed in the early 1970s). However, the Segel model is fairly easy to use and useful for the planned tests.

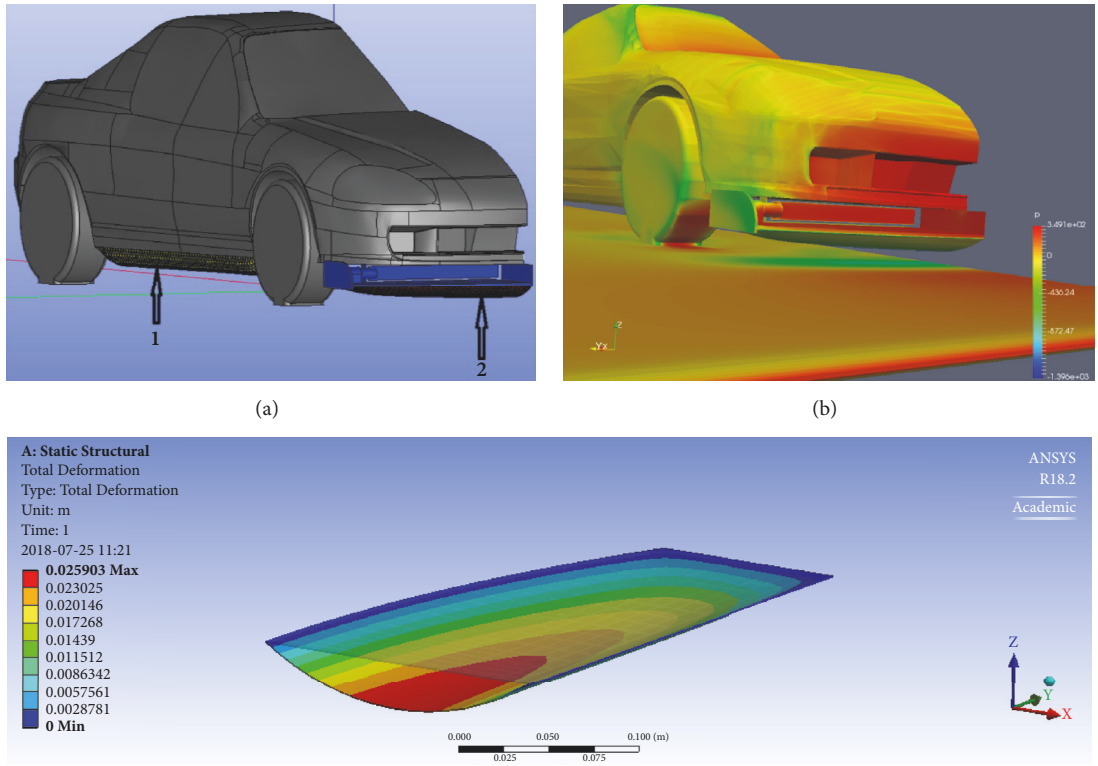

FIGURE 14: (a) Car with additional aerodynamic elements. The splitter is marked blue. Number 1 is a pneumatic side curtain. Number 2 is the airbag under the splitter. (b) An example of simulation results obtained using the OpenFOAM program. (c) Deformation of the airbag under the splitter. Numerical simulation carried out using the ANSYS program.

It is a function of the slip angle, cornering stiffness, tire vertical load, friction coefficient, and longitudinal force. A 6DOF model takes into account the possible rotation of the car body along the main 3 axes as well as vertical and horizontal body motion. This takes into account the lateral forces generated during acceleration and braking, defines the tire road contact forces, lateral forces and slip angles influenced by additional aerodynamic forces generated by movable aerodynamic elements. The action of suspension stabilizers is also taken into account. The scheme of forces and body movement definition is shown in Figure 15. The algorithm was coded in Fortran 95.

The software delivers information about the temporal car body position (rolling; pitching), tire slip angles, and forces. It can help develop algorithms for the electronic control system to steer the movable aerodynamic elements. Figure 16(a) depicts the variation of the longitudinal and lateral acceleration during cornering with an initial speed of 50 m/s, the "low aero" corresponds to a drag coefficient equal to 0.40 and the lift coefficient equal to −0.45, whereas the "high aero" corresponds to a drag coefficient equal to 0.75 and the lift coefficient equal to −0.75. The steering wheel changes the angle of the front wheels sinusoidally in 2 seconds from 0° to 15°.

Figure 16(b) presents some results showing differences in car motion with and without the action of the aerodynamic elements. The observed car motion is characteristic for a case with high slip angles on the rear tires which cause oversteer when the aerodynamic downforce is not sufficient ("low aero"), when the aerodynamic load is high enough the balance of the car changes to neutral ("high aero"). This proves that relatively small changes in car dynamics can generate large changes in car position.

Each of the models and solutions presented so far were created separately without a direct two-way interaction between the fluid flow and the car body dynamics. Knowing the results of the investigation of coupled FSI problems [19], the simultaneous simulation of flow problems connection with car body motion caused by aerodynamic forces was also undertaken.

3.7. Coupled FSI Simulation of the Car Braking Process Assisted and Strengthened by Movable Aerodynamic Elements: Fully Coupled Analysis of the Braking Process. Designing lighter cars with lower drag coefficients requires an assurance of car stability in all road conditions. In simulations, it is rather rare to take into account coupling between car dynamics and aerodynamics. Very often, it is assumed that car movement will not affect aerodynamic forces. As shown in [2], this assumption is not correct. The authors showed that including bidirectional fluid structure interaction can lead to significant changes in aerodynamic forces.

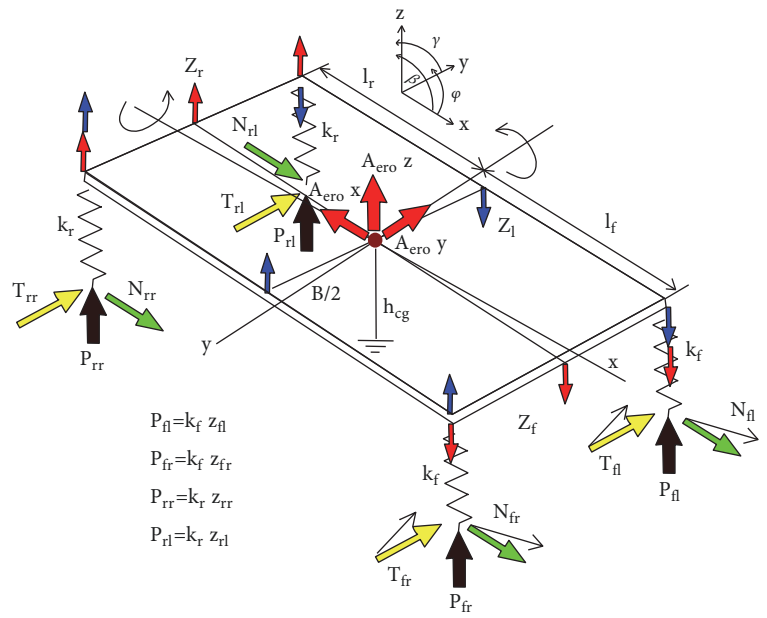

FIGURE 15: Scheme of forces and body movement definition.

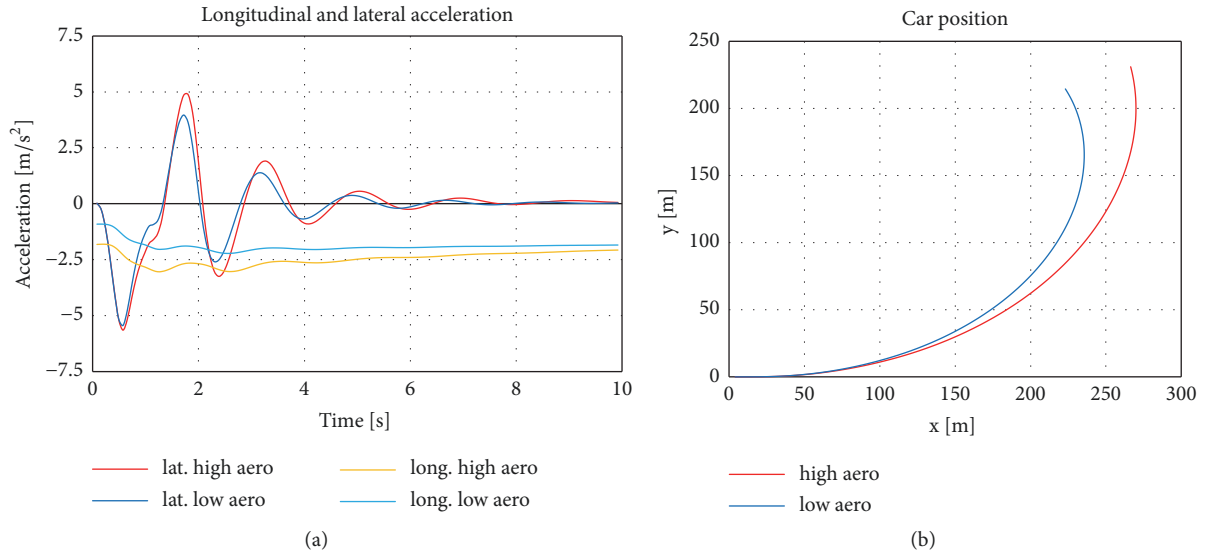

FIGURE 16: (a) Variation of the longitudinal and lateral acceleration during cornering. (b) Car position influenced by the aerodynamic forces.

The physics is complicated during the car braking process. A braking car generates a transfer of load to the front axis (see Figure 17), pressing the suspension springs and changing the inclination of the body resulting in a change of aerodynamic forces. During braking, the car slows down and this reduces the aerodynamic forces again thus changing the car body position. This is a fully coupled FSI process which had to be modeled and simulated.

In the case of braking (or accelerating), the car body pitches due to the elastic suspension system and the acting inertia forces. The pitch angle can be treated as an angle of attack for the car body. At the same time, the clearance between the car and the ground also changes. Figure 17 illustrates the possible configurations. This situation causes a change in the pressure distribution over the entire body. Furthermore, a change in pressure distribution affects the pitch angle and clearance. In other words, there is a strong coupling between the car behavior and the aerodynamic forces.

In this research, fully coupled analyses were performed to check if it is possible to predict car dynamic behavior during braking. The obtained results were validated against a full car experiment as described in Section 3.3. Currently, very few of the published papers refer to a fully coupled

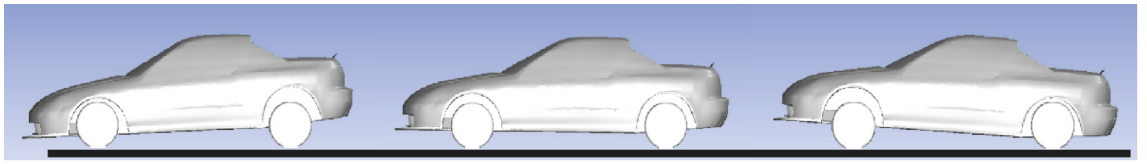

Figure 17: Pitching of the car body due to the elastic suspension system during braking or acceleration.

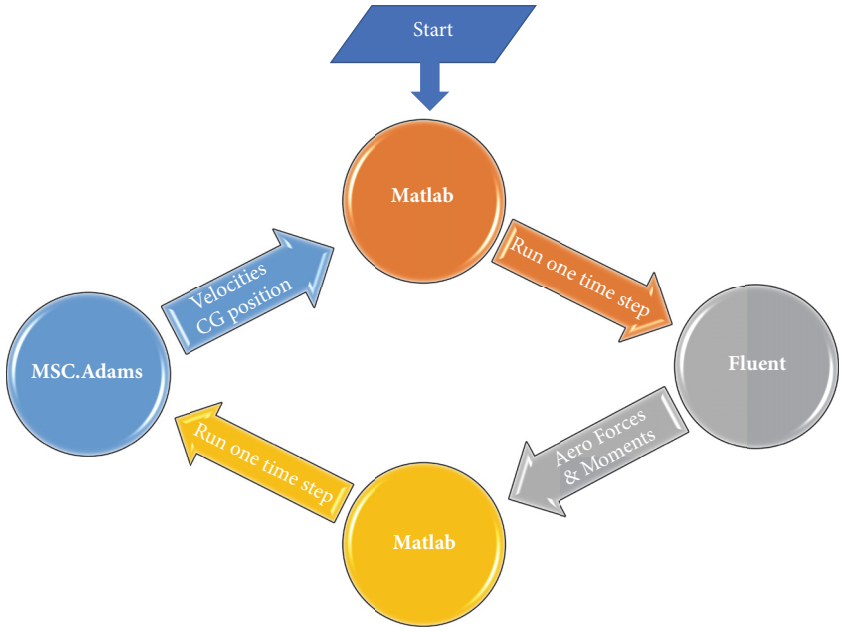

Figure 18: Scheme of the connections of the programs and exchange of data.

car analysis in which the vehicle speed significantly varies over time (such as during the acceleration/braking process). The method presented in this study to simulate the braking process utilizes a combination of high-end software for CFD modeling (Ansys® FLUENT®), vehicle dynamics (MSC.ADAMS/Car®), and a block diagram environment for multidomain simulation (MATLAB/Simulink®) which acts as an interface to exchange data between the first two tools. To allow communication with FLUENT®, it is launched in "as-a-server" mode. This option creates a COM port which enables remote connection to and control of FLUENT® sessions from an external application. Connection to MSC.ADAMS® is achieved via the "Adams Plant" option. On the Matlab side, dedicated Level 2 S-Functions were created. These functions are responsible for driving the CFD and dynamics analyses. The data workflow is presented in Figure 18.

The coupling procedure was validated against the wind tunnel experimental data. In this case self-excited vibration of square beam in crossflow was used. The set-up of the test stand is presented in Figure 11(a). Corresponding models were built for CFD and dynamic analyses (Figure 11(b)). The obtained results show that frequency and amplitude were captured with a high level of accuracy. With a validated coupling mechanism and the selected turbulence model – k-ω SST – which assures a good correlation to the wind tunnel (see Section 3.3), a coupled analysis of the full car dynamics was performed.

During the research, it was concluded that the reference frame needed to be changed to simulate velocity change in the CFD analysis. Instead of a classical reference frame with an observer at rest, the reference frame with a moving observer was used. In this case, the whole computational domain was moved during the analysis with velocity which varies over time. The car instantaneous speed is calculated using MSC.Adams/Car®. The overset mesh was used to allow the movement of the car body and additional aerodynamics surfaces. The split into subdomains was performed according to elements which can be moved independently (car body, wheels, and rear airfoil). Based on the grid convergence study, for the steady state case, the hybrid hexa/polyhedra mesh used contained 7.7 million elements. Flow symmetry was assumed and a half car model was used. The analysis was performed in double precision, and the second-order spatial discretization schemes were used. The full car MSC.Adams® dynamic model (Figure 19) was fed with the measured data: suspension stiffness and damping nonlinear characteristics.

Mass properties were estimated based on "Measured vehicle inertial parameters" by NHTSA [20]. Friction coefficient between the tires and the road was set to 0.71 which corresponds to dry road conditions and is in line with the

Table 2: A comparison of the numerical and experimental data.

Value	Unit	Experiment	Analysis	Difference	%
Traveled Distance	m	111	112	1	0.90
Time to Stop	s	5.34	5.29	0.05	−0.94
Max Deceleration	g	1.0	0.95	0.05	−5

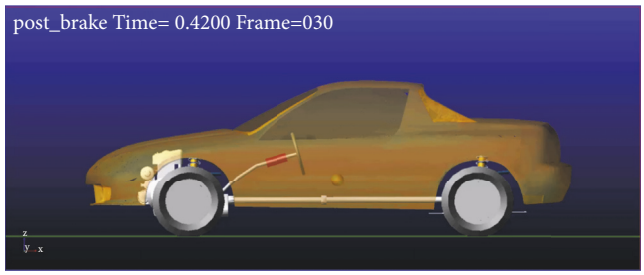

Figure 19: MSC.Adams/Car model used in the analysis.

Jones and Childers report [21]. The initial velocity for braking was 40.31 m/s (145 km/h). Based on [15], it was assumed that 0.5 s is needed to achieve full braking torque after the decision for emergency braking. The rear airfoil in the investigated configuration was in position "zero". Figure 20(a) shows the pressure distribution on the car body and the isosurface of Q-Criterion colored with velocity magnitude at the starting point for braking.

The obtained braking characteristics presented in Figure 21 show a good agreement between the numerical prediction and the experimental data. The discrepancy in the traveled distance and time to stop is less than 1%. The mismatch in maximum deceleration is 5%. However, this value can be affected by the irregular shape of the experimental characteristic. A summary of the results is presented in Table 2.

The current research activities also focused on cornering analysis. The aim of this part of the study was to check the impact of aerodynamic configuration on cornering critical speed. It was necessary to switch the reference frame to a moving observer. With such an approach it was possible to simulate cornering and take into account all car movements associated with this maneuver. Figure 20(b) presents the initial CFD solution for quasi steady condition. It is clearly visible that flow symmetry is broken, especially on the rear part of the car body.

4. Road Tests

The final part of the presented study includes real vehicle road tests performed on a Honda CRX del Sol with some custom modifications. The test took place on a training track which was suitable for evaluating how the designed active control system can enhance emergency car maneuvers that sometimes need to be performed while driving on city roads. The radius of the curves and the length of the longest straight were insufficient to test the scenarios of emergency maneuvers during a very high-speed drive which could occur on a highway. It should be noted that the aerodynamic forces aiding the drive were limited by the fact that lower ranges of speed were achieved during the tests. The test car was driven by an experienced rally driver, Arkadiusz Nowikow, whose driving technique made it possible to complete all test scenarios in a highly repetitive manner. He also gave invaluable insight about the car's handling and its change with different aerodynamics and suspension settings. The passenger of the car who was also the operator of the control system when it was tested in semiautomatic mode was a source of information about the driving comfort. In this way, the data acquired by the sensors was enriched by subjective human experiences.

The active aerodynamic elements mounted on the rear side of the test car can be seen in Figure 22. They include a pair of moving wings and spoilers which can work independently and enable an asymmetrical configuration to be set. The active suspension and the aerodynamics play an important role in the distribution of force while the vehicle is moving. The system described in Section 2 was developed and thoroughly tested. Part of the data acquired is presented below.

With known values of the aerodynamic forces, which depend on the flow around the vehicle and knowledge of the vehicle dynamics, a set of track tests was conducted. The control and acquisition system was tested by means of active aerodynamic and suspension control for predefined scenarios, as well as being controlled, in a dynamic way, by software algorithms. Several different scenarios were executed during the track tests which included rapid braking, slalom and tight turns. For a braking scenario, detection of the braking pedal being pushed was the onset value of the aerodynamic brake activation, the rear wing and spoilers were set to the maximum angle of attack to maximize drag produced by the car body. Slalom involved slight adjustments of the rear wings that could be undertaken in split seconds before the turning direction was changed to the other side. For the scenario of driving into a tight curve, the system was activated when the values of the side (Y component) acceleration (see Figure 23) as well as the angular position of the steering wheel exceeded predetermined values. In this case, the active aerodynamic elements were configured to maximize the downforce on the car's side closer to the inside of the curve, whereas the aerodynamic properties of the other side of the car remained neutral. Additionally, the suspension on the outer side was stiffened to limit the negative effects caused by body roll.

A comparison of two configurations is presented in Figure 24 and Figure S1. The red color is data for the configuration with active aerodynamics and active suspension turned on, whereas the blue data is for static positions of the

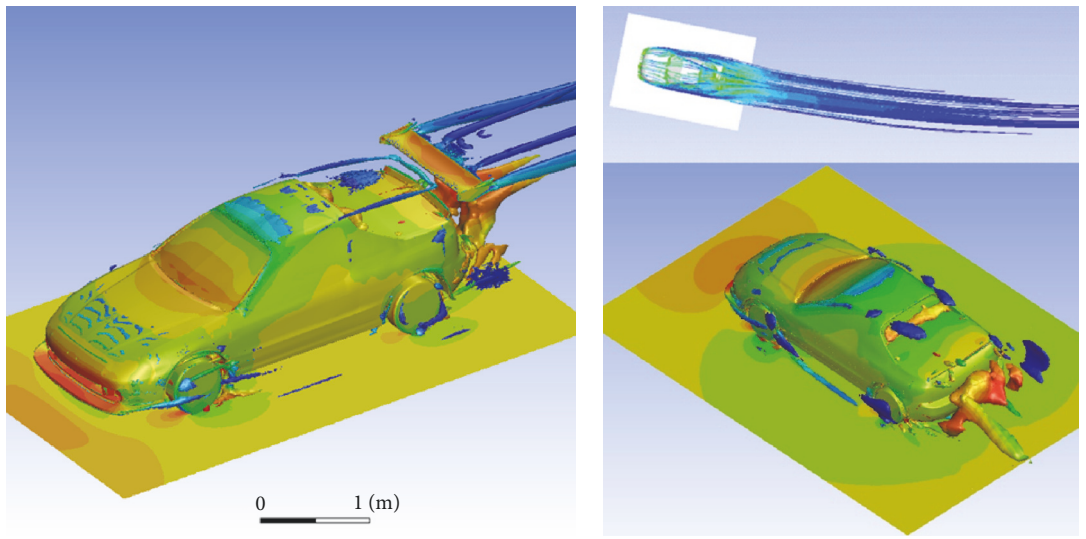

(a) (b)

Figure 20: (a) Starting point for braking analysis. Car body colored with static pressure and iso-surface of Q-Criterion colored with velocity magnitude. (b) Initial CFD results for cornering analysis. Streamlines colored with velocity magnitude (upper) and static.

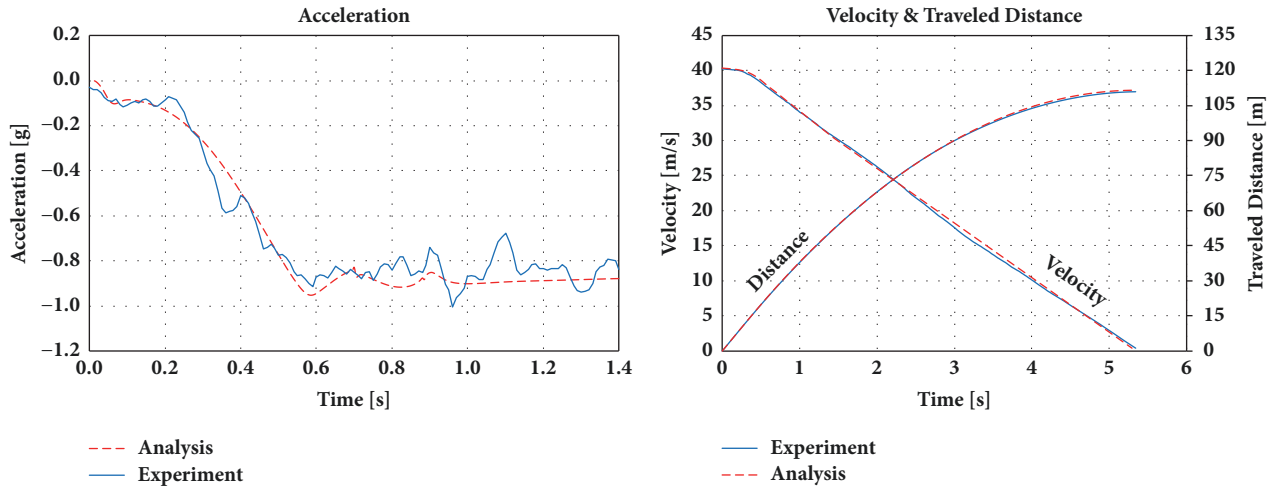

Figure 21: A comparison of the data from the simulations and the road tests.

Figure 22: Snapshot from a test drive with the active aerodynamics deployed, where Lw/Rw – active left/right wing, Ls/Rs – active left/right spoiler.

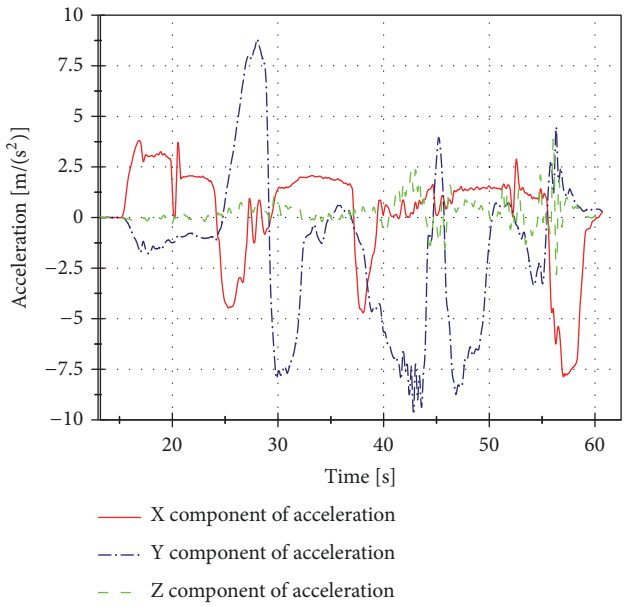

Figure 23: Set of data obtained from acquisition system, vehicle acceleration plot.

aerodynamic surfaces. Selected data, such as speed, lateral acceleration, steering wheel position and suspension deflection is presented in Figure 24, whereas the data presented in Figure S1 is supplemented by the GPS position noted on the map. Moreover, the gathered data also included information about throttle, braking, pitch, yaw and roll angles, as well as settings of the suspension stiffness and the aerodynamic surfaces configurations.

The data obtained from the tests made it possible to verify all of the preceding stages of the work. The track test can specify those points where, for example, the theoretical assumptions, the road conditions (roughness) and wind tunnel results were not enough to maintain a steady equilibrium and the assumed conditions. In Figure 24(b), it can be seen that, for the red line, the Y component of acceleration changes have an oscillatory character, which means that the car's suspension is at its limit. In other words, the car is moving in the manner of small jumps in a direction perpendicular to the driving direction. Moreover, it is clearly noticeable that there is a difference in the velocity reached at the fastest corner, with the configuration using active aerodynamics having the highest velocity.

5. Conclusions

The realization of the optimal design of the geometry and control system of movable aerodynamic devices increasing the safety of fast moving cars requires multidisciplinary synchronized action correlating the weak and strong points of the considered solutions.

This paper presented a range of methods of modeling and simulating different aspects of controlling car aerodynamic characteristics by actuating movable aerodynamic adds-on on the car body to increase the traction, braking and lateral force in road conditions requiring such action. The reaction time required by the flow structure to change after a change of the car body geometry is an important factor. On the one hand, mechanical elements require fast movement but on the other hand the flow around the car body needs time to accommodate the new flow conditions. Different physical processes exist simultaneously in the considered problem and, especially, FSI problems required the use of different software for modeling and simulation.

The synchronized action of specialists in unsteady flow simulations, flexible material FSI simulations, car dynamic simulations, coupled FSI car aerodynamics and car dynamics, experimental tests in wind tunnel, and road tests can lead to a solution of electronically controlled movable aerodynamic elements activated and controlled in a manner to extend the driving limits of fast cars.

Data Availability

Data in the form of figures and tables that support the findings of the numerical calculations presented in this study are included within the article. Data acquired during the track tests are included within the article as well as within the supplementary information files.

Conflicts of Interest

The authors declare that they have no conflicts of interest.

Acknowledgments

The project was financed by the National Center for Research and Development (Narodowe Centrum Badań i Rozwoju) as part of the project entitled "The Active System of Car Body Oscillation Damping", Grant no. PBS3/B6/34/2015.

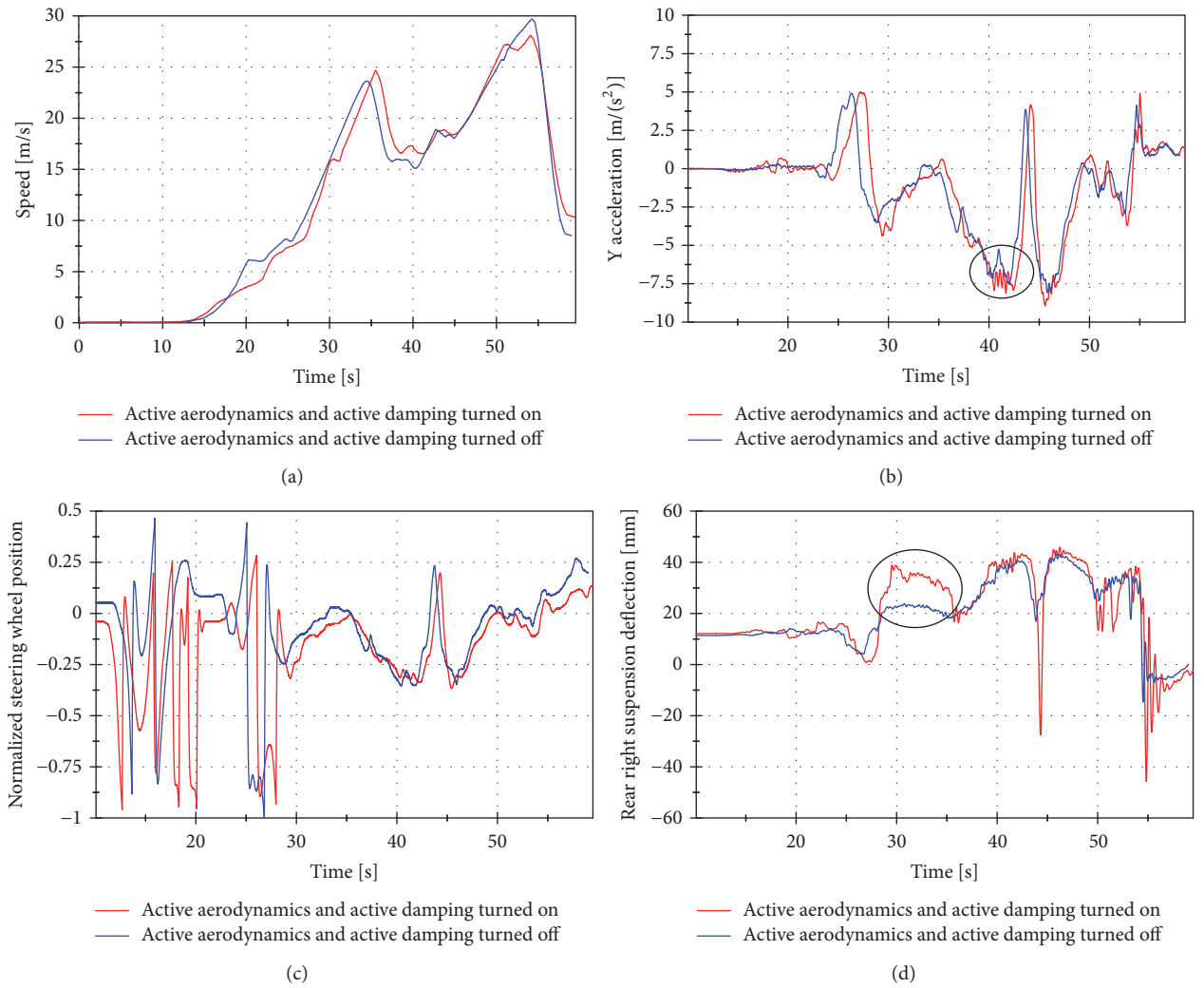

FIGURE 24: (a) Speed. (b) Lateral acceleration. The suspension instability is marked with a circled area. (c) Steering wheel position. (d) Rear right suspension deflection. The differences in the deflections are marked with a circled area.

Supplementary Materials

The supplementary material consists of a movie called "track_test_data.mp4" which is sample data acquired during the track test drive; one time frame from this movie is presented in Figure S1. The movie contains plots of such data as speed, lateral acceleration, steering wheel position, and suspension deflection, matched with the car's position on the test track. *(Supplementary Materials)*

References

[1] ISO 12021:2010, *Road Vehicles – Sensitivity to Lateral Wind – Open-Loop Test Method Using Wind Generator Input*, 2010, https://www.iso.org/standard/53602.html.

[2] D. C. Forbes, G. J. Page, M. A. Passmore, and A. P. Gaylard, "A Fully Coupled, 6 Degree-of-Freedom, Aerodynamic and Vehicle Handling Crosswind Simulation using the DrivAer Model," *SAE International Journal of Passenger Cars—Mechanical Systems*, vol. 9, no. 2, 2016.

[3] G. Wahl, "918 Spyder – the impulse source for future sports car concepts," in *Proceedings of the 5th International Munich Chassis Symposium 2014*, pp. 35–56, Springer Fachmedien, Wiesbaden, Germany, 2014.

[4] A. Eskandarian, *Handbook of Intelligent Vehicles*, Springer, 2012, https://scholar.google.pl/scholar?hl=pl&as_sdt=0%2C5&q=%22Handbook+of+Intelligent+Vehicles%22+Azim+Eskandarian&btnG=.

[5] W. Jarisa, "FUTURE TECHNOLOGY – Road condition classification using information fusion," in *Proceedings of the 7th International Munich Chassis Symposium 2016*, pp. 939–957, Springer Fachmedien, Wiesbaden, Germany, 2017.

[6] X. Qu, F. Yu, and S. Zhao, "Research on Curve Safety Speed Warning for Vehicle with Risk Prediction," in *Proceedings of SAE-China Congress 2016: Selected Papers*, vol. 418 of *Lecture Notes in Electrical Engineering*, pp. 431–445, Springer, Singapore, 2017.

[7] M. Fainello, "Optimizing passive vehicle dynamics for active safety and autonomous driving," in *Proceedings of the 8th International Munich Chassis Symposium 2017*, pp. 243–251, Springer Fachmedien, Wiesbaden, Germany, 2017.

[8] H. Beglerovic, A. Ravi, N. Wikström, H. Koegeler, A. Leitner, and J. Holzinger, "Model-based safety validation of the automated driving functio highway pilot," in *Proceedings of the 8th International Munich Chassis Symposium 2017*, pp. 309–329, Springer Fachmedien, Wiesbaden, 2017.

[9] M. Abramowicz, K. Kamieniecki, A. Piechna, and P. Rubach, "Using ANSYS and SORCER Modeling Framework for the Optimization of the Design of a Flapping Wing Bionic Object," *Mach. Dyn. Res*, vol. 39, pp. 21–36, 2015.

[10] J. Katz, *Race Car Aerodynamics: Designing for Speed*, Bentley (Robert) Inc, Cambridge, UK, 2nd edition, 1996.

[11] F. R. Menter, "Two-equation eddy-viscosity turbulence models for engineering applications," *AIAA Journal*, vol. 32, no. 8, pp. 1598–1605, 1994.

[12] C. Fu, M. Uddin, and A. C. Robinson, "Turbulence modeling effects on the CFD predictions of flow over a NASCAR Gen 6 racecar," *Journal of Wind Engineering & Industrial Aerodynamics*, vol. 176, pp. 98–111, 2018.

[13] J. Katz, *Automotive Aerodynamics*, Wiley, 2016.

[14] J. Piechna, T. Janson, P. Sadowski, S. Tudruj, A. Piechna, and L. Rudniak, "Numerical study of aerodynamic characteristics of sports car with movable flaps and deformable airbags," in *Proceedings of the Automotive Simulation World Congress*, 2013.

[15] M. Mitschke, *Car Dynamics*, Transport and Communication Publishers, 1st edition, 1977.

[16] M. Guiggiani, *The Science of Vehicle Dynamics: Handling, Braking, and Ride of Road and Race Cars*, Springer, the Netherlands, 2014.

[17] G. Genta, *Motor vehicle dynamics: modeling and simulation*, World Scientific, 1997.

[18] R. Rajamani, *Vehicle Dynamics and Control*, Springer US, Boston, Mass, USA, 2012.

[19] T. Janson and J. Piechna, "Numerical Analysis of Aerodynamic Characteristics of a of High-Speed Car With Movable Bodywork Elements," *Archive of Mechanical Engineering*, vol. 62, no. 4, pp. 451–476, 2015.

[20] G. J. Heydinger, R. A. Bixel, W. R. Garrott, M. Pyne, J. G. Howe, and D. A. Guenther, "Measured Vehicle Inertial Parameters-NHTSA's Data Through November 1998," in *Proceedings of the International Congress & Exposition*, pp. 10–4271, 1999.

[21] E. R. Jones and R. L. Childers, *Contemporary College Physics*, McGraw Hill, 2001.